Computational Micromechanics Modeling of Piezoresistivity of Carbon Nanotube Polymer Nanocomposites

Xiang Ren[1], Gary D. Seidel[2*]

[1,2]*AOE department, Virginia Tech, Blacksburg, VA, USA, 24061*
**gary.seidel@vt.edu*

Keywords: Nanocomposites, Piezoresistivity, Micromechanics, FEM.

Abstract
It has been observed that carbon nanotubes (CNT) have a measurable inherent piezoresistive effect, that is to say that changes in carbon nanotube strain can induce changes in its resistivity, which may lead to observable macroscale piezoresistive response of nanocomposites. In this paper, the focus is on modeling the effect of inherent piezoresistivity of carbon nanotubes on the nanocomposites piezoresistive behavior by using computational micromechanics techniques based on finite element analysis. The computational results show the magnitude of the piezoresistive coefficients needed for the piezoresistive response of the macroscale nanocomposites to be comparable with experimental data in the literature if inherent piezoresistive effect of CNTs is the only driving force for the piezoresistive response of the macroscale nanocomposites.

1 Introduction
Multifunctional hybrid composites being considered for use in hypersonic vehicles can consist of a gradual transition from ceramic to metallic to fiber reinforced polymer layers, with each layer having tailored functionalities. Within the latter, there is interest in the development of a structural health functionality based by using nanocomposite interphase regions in the fiber reinforced polymer layer for deformation and damage detection via fuzzy fibers. To date, several types of CNT-polymer nanocomposites have been shown to have linear piezoresistive responses with small loadings of single-walled carbon nanotubes (SWCNT) or multi-walled carbon nanotubes (MWCNT)[1, 2, 3, 4, 5]. Such piezoresistive properties make CNT-polymer nanocomposites very attractive in the manufacturing of high gauge-factor low-voltage strain gauges. In addition, CNT-polymer nanocomposite strain gauges have the potential to be directly embedded in structural composites during composite processing to provide internal strain sensing in contrast to the customary surface strain measurements obtained from commercial strain gauges bonded to the surface of structures. While there is ample experimental evidence demonstrating the piezoresistive response of nanocomposites, the mechanisms governing piezoresistivity of nanocomposites are less clear in terms of relative magnitude and interactions. In order to aide in the design of piezoresistive nanocomposite strain gauges with tailored sensitivities, it is necessary to develop an understanding of the underlying mechanisms at the micro and nanoscales which govern the macroscale piezoresistive response.

At present, several mechanisms are believed to contribute to the piezoresistive response of CNT-polymer nanocomposites. Kang et al.[3] have indicated that the piezoresistive response of macroscale nanocomposite material originates from the tunneling effect[6] between conducting inclusions (CNTs) at the nanoscale under compression or tension. Patrik

et al.[7] indicated that the geometric change of the specimen may have an effect on its macroscale resistance behavior. An additional mechanism is associated with the CNTs themselves which have been shown to have a considerable inherent effect that cannot be neglected. It has been observed both experimentally and in modeling that mechanical deformation of CNTs can directly lead to significant changes in their conductance[8, 9, 10, 11, 12, 13], indicating CNTs are themselves good strain sensors due to inherent piezoresistivity.

The focus of the present work is on studying the macroscale piezoresistive behavior of CNT-polymer nanocomposites due to the inherent piezoresistivity of CNTs in the absence of other factors such as the electric tunneling effect between CNTs. A computational micromechanics model based on finite elements analysis is developed and used to determine the changes in macroscale resistance (i.e. effective macroscale piezoresistance) due to changes at the nanoscale associated with CNT deformation and inherent piezoresistivity. The effects of CNT geometry, local volume fraction, and inherent piezoresistive coefficients on the macroscale piezoresistivity are studied parametrically. The results are discussed in the context of experimentally observed gauge factors for nanocomposites and the strength of electromechanical coupling needed to achieve observed responses.

2 MODEL DESCRIPTION

2.1 Multiscale model for the CNT-polymer nanocomposites

Typically, the dispersion and shape of CNTs in the CNT-polymer nanocomposites may be complicated, e.g. the CNTs can be curved along their axes, randomly oriented, and bundled with the other CNTs. The modeling of the piezoresistive response of the nanocomposites in the continuum domain with complicated microstructures would not be an easy task, and therefore for the purposes of the present work we will focus on a simplified microstructure representation. As shown in Fig. 1, a multiscale idealization is applied for the nanocomposites, in which the CNTs are well-dispersed, aligned and perfectly bonded to the surrounding polymer. The nanoscale RVE is chosen to represent the macroscale nanocomposites, for which the effective piezoresistive response can be modeled by solving boundary value problems on the nanoscale RVE.

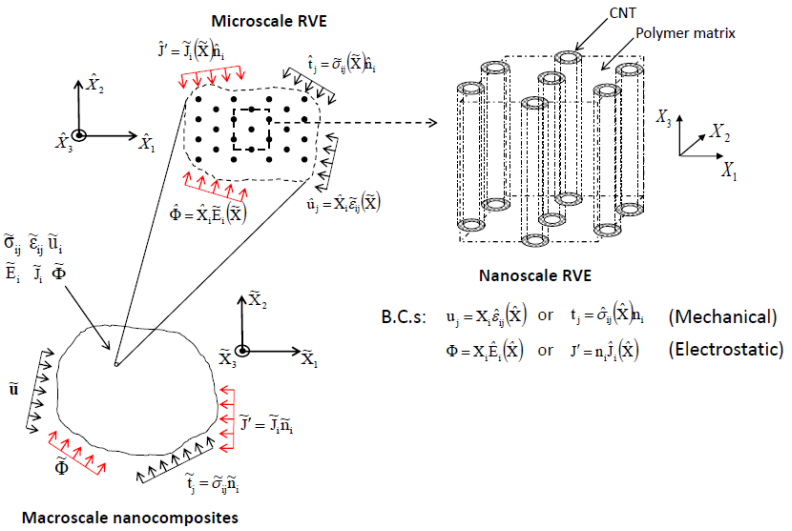

Figure 1. The hierarchical multiscale modeling of the nanocomposites, in which there are well-dispersed and aligned CNTs

2.2 2D nanoscale RVEs for the nanocomposites

The 3D nanoscale RVE for aligned CNT nanocompoistes (Fig. 1) can be reduced to two 2D RVEs in order to save computational time. As seen in Fig. 2(a), due to high aspect ratios (>200) of CNTs, the transverse properties of the nanocomposites are typically modeled using the regular hexagonal array RVE under in-plane strain assumption. The annulus areas represent the cross-sections of CNTs, and the remaining area is pure polymer matrix. Correspondingly, a plane strain periodic finite element model is constructed to model the piezoresistive response of the nanocomposites in the transverse directions. On the other hand, for cases where the loading is axisymmetric, for example in the uniaxial tension test, the axial properties of the nanocomposites are modeled by using a 2D axisymmetric RVE that is axisymmetric about the axis (Fig. 2(b)). The highlighted area is CNT, and the remaining area is pure polymer matrix. Correspondingly, an axisymmetric finite element model is constructed to model the axial piezoresistive response of the nanocomposites.

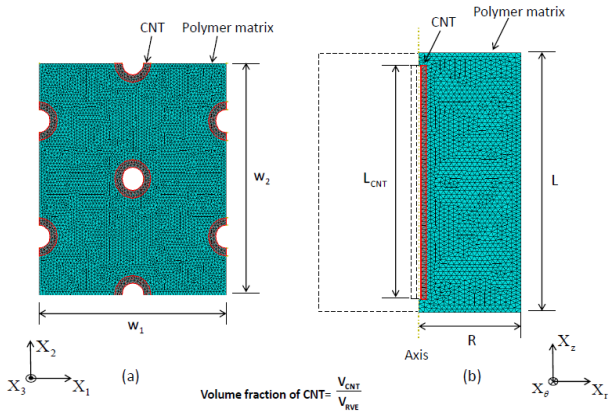

Figure 2. Nanoscale RVEs for the nanocomposites with well-dispered and aligned CNTs. (a) is the transverse hexagonal nanoscale RVE with the volume fraction of the CNTs being 10%. (b) is the axisymmetric nanoscale RVE with the volume fraction of the CNT being 0.5% and the aspect ratio of the CNT being 20 (The aspect ratio used here is only for showing purposes, the real aspect ratio used in the computations is much higher). X_1 and X_2 are in the same plane as X_r and X_θ. W_1 is the width of the hexagonal nanoscale RVE in X_1 direction, W_2 is the width of the hexagonal nanoscale RVE in X_2 direction, L is the length of the axisymmetric nanoscale RVE in X_z direction, L_{CNT} is the length of the CNT, and R is the half distance between two adjacent CNTs.

2.3 Governing piezoresistive equations for the multiscale model

For pure polymer matrix, there is no piezoresistive effect, however for CNTs, due to the inherent piezoresistive effect, the change in resistivity is coupled with the strain in the CNT, such that the instantaneous resistivity of the CNT can be expressed as:

$$\rho_{ij}^{C} = \rho_{ij}^{C0} + \Delta\rho_{ij}^{C} \tag{1}$$

in which ρ_{ij}^{C0} are the initial zero strain resistivities of the CNT, and $\Delta\rho_{ij}^{C}$ are the change in resistivities induced by inherent piezoresistive effect of the CNT. The inherent piezoresistive effect of CNTs can be denoted as below:

$$\Delta\rho_{ij}^{C} = g_{ijkl}^{C}\varepsilon_{kl} \tag{2}$$

The g_{ijkl}^{C} are the piezoresistive strain coefficients of the CNT.

In order to compare with measures more commonly used in experiments, the effective resistivity ρ_{zz}^{Eff} obtained in the tension tests can be further converted to the macrsocale nanocomposite gauge factor by using the equation below:

$$G = \frac{\frac{\Delta R}{R}}{\varepsilon} = \frac{\frac{\rho^f \frac{L^f}{A^f} - \rho^0 \frac{L^0}{A^0}}{\rho^0 \frac{L^0}{A^0}}}{\varepsilon} = \frac{\frac{\rho^f}{\rho^0}\frac{1+\varepsilon}{(1-\nu\varepsilon)^2} - 1}{\varepsilon} \quad (3)$$

in which G is the effective gauge factor of the nanocomposites G^{Eff}, ρ^0 is the effective resistivity of the nanocomposites without strain, ρ^f is the effective resistivity of the nanocomposites with applied macroscale tension ε_0, and ν is the effective Poison's ratio, which can be obtained from the mechanical stress and strain within the nanoscale RVEs[14] or by using the composite cylinder method[15].

3 RESULTS AND DISCUSSION

The polymer matrix used in the model is the epoxy resin EPON 828 which is assumed to be isotropic linear elastic below its glass transition temperature. The detailed mechanical, electrical and geometric parameters of the CNT and EPON 828 are listed in Table 1:

Properties / Materials	Geometry	Mechanical	Electrical
Single-walled CNT	R_{Out}=0.85nm R_{In}=0.51nm	$E = 1100Gpa$ $\upsilon = 0.14$	$\kappa = 10^5 S/m$
EPON 828	Volume fraction $= 1 - \frac{V_{\text{CNT}}}{V_{\text{RVE}}}$	$E = 3.07Gpa$ $\upsilon = 0.3$	$\kappa = 1.49 \times 10^{-9} S/m$

Table 1. Mechanical, electrical and geometric parameters for the CNT and EPON 828 polymer matrix[14, 16, 17, 18, 19]. The conductivity of the CNT listed here is the initial conductivity with zero strain.

In the present work, parametric study is undertaken on the gauge factors of the CNT, and the conversions from gauge factors to axial piezoresistive strain coefficients g_{zz}^C are listed in Table 2:

Case#	G^C	$\rho^0\ (\Omega \cdot m)$	ν_{rz}^C	$g_{zz}^C\ (\Omega \cdot m)$
1	3E3	1E-5	0.14	2.96E-2
2	1E6	" "	" "	9.87E0
3	1E11	" "	" "	9.87E5
4	1E14	" "	" "	9.87E8
5	1E17	" "	" "	9.87E11

Table 2. The conversions from the gauge factor of the CNT (G^C) to its axial piezoresistive strain coefficient g_{zz}^C at the strain ε_c = 1%. It can be noted that the gauge factor of the CNT in case 1 is close to the results found in experiments, and the gauge factors of the CNT in other cases are hypothesized for the purposes of parametric study. For each case, the g_{zz}^C is used as a constant parameter (i.e. is strain, temperature and voltage independent), and it is assumed that all other g_{ij}^C are zero.

On the other hand, the majority of data regarding inherent piezoresistivity of CNTs is limited to axial testing. As such, there is little data available regarding the remaining four independent

piezoresistive strain coefficients need to fully characterize the transversely isotropic piezoresistive response of the CNT. In order to demonstrate the application of the piezoresistive algorithm, the hypothesized transverse piezoresistive strain coefficients are provided in Table 3:

Case#	Type of Case	Non-zero Piezo strain coefficients
1	Uniaxial tension	$g_{11}^{C} = g_{22}^{C} = 10^{10}\Omega\cdot\mathrm{m}$
2	Uniaxial tension	$g_{11}^{C} = g_{22}^{C} = 10^{11}\Omega\cdot\mathrm{m}$
3	Uniaxial tension	$g_{11}^{C} = g_{22}^{C} = 10^{12}\Omega\cdot\mathrm{m}$
4	Uniaxial tension	$g_{11}^{C} = g_{22}^{C} = 10^{13}\Omega\cdot\mathrm{m}$
5	Uniaxial tension	$g_{11}^{C} = g_{22}^{C} = 10^{14}\Omega\cdot\mathrm{m}$
6	Biaxial tension	$g_{11}^{C} = g_{22}^{C} = 10^{10}\Omega\cdot\mathrm{m}$
7	Biaxial tension	$g_{11}^{C} = g_{22}^{C} = 10^{11}\Omega\cdot\mathrm{m}$
8	Biaxial tension	$g_{11}^{C} = g_{22}^{C} = 10^{12}\Omega\cdot\mathrm{m}$
9	Biaxial tension	$g_{11}^{C} = g_{22}^{C} = 10^{13}\Omega\cdot\mathrm{m}$
10	Biaxial tension	$g_{11}^{C} = g_{22}^{C} = 10^{14}\Omega\cdot\mathrm{m}$

Table 3. The hypothesized transverse piezoresistive strain coefficients of the CNT. For each case, the g_{ij}^{C} that are not listed are zero.

3.1 Results for the transverse directions of the nanocomposites

The effective resistivity ρ_{22}^{Eff} of the hexagonal nanoscale RVE of each load step can be obtained by applying a potential difference across the X_2 direction, so that the effective resistivities ρ_{22}^{Eff} of the 10 cases with the change of boundary strain can be obtained and are shown in Fig 3. It can be seen that as the piezoresistive strain coefficients g_{11}^{C} and g_{22}^{C} increase from $10^{10}\ \Omega\cdot\mathrm{m}$ to $10^{14}\ \Omega\cdot\mathrm{m}$, the curves for the effective resistivity tend to change from linear to nonlinear with increase applied boundary strain. This transition is attributed to the aforementioned transition from a conductive fiber in a non-conductive matrix arrangement of the zero-strain and low g_{ij}^{C} cases to a non-conductive fiber in a "conductive" matrix arrangement for larger g_{ij}^{C}. It is observed that the effective resistivity of the nanocomposite is governed by the least conductive (highest resistance) phase. Thus, when the matrix governs effective resistivity, the changes in nanotube resistivity are marginalized and fit will be with a rule of mixtures for resistivity which is already largely saturated by the matrix resistivity. However, when the CNT resistivity governs the effective response, relationship can be thought of as more like the inverse rule of mixtures and therefore non-linear.

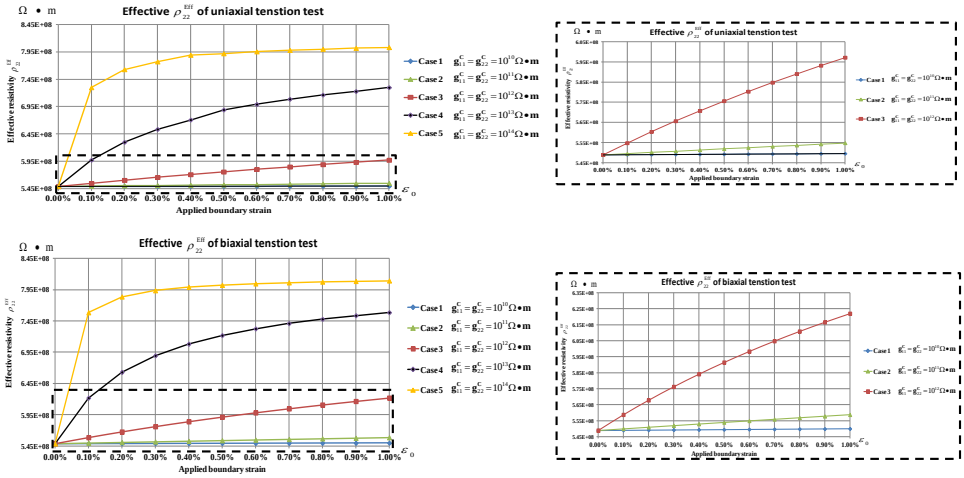

Figure 3. The plot of the effective resistivity of the RVE with the increase of the macroscale boundary strain. (a) and (b) are the results for the cases of the plane-strain uniaxial tension test, and (c) and (d) are the results for the cases of the plane-strain biaxial tension test.

As observed in Table 4, by applying Eq. (3) the effective gauge factor of the macroscale nanocomposites measured in the plane-strain uniaxial tension test can be obtained and demonstrates a nearly strain independent response for the case 1 and 2 (indicating a linear gauge factor) and increasingly strain dependent response for cases 3, 4 and 5 (indicating a non-linear gauge factor). Notice that herein only inherent piezoresistive effect of CNTs is considered, and the inherent piezoresistive strain coefficients of CNTs are hypothesized for the purpose of parametric study. From literature review, it is found the gauge factor measured in the axial direction of the strain gauge that made of randomly oriented CNTs is from 0.48 to 5 [2, 3, 4, 5], compared with the gauge factors obtained here, it can see that they roughly lies in the same level as the 1st and 2nd cases.

Case#	0.1%	0.4%	0.7%	1%
1	1.67	1.68	1.68	1.68
2	2.65	2.65	2.65	2.65
3	12.22	11.57	11.00	10.49
4	89.56	57.34	43.56	35.03
5	331.53	111.65	67.09	48.60

Table 4. The effective gauge factors measured in the transverse direction of the strain gauge made of CNT-polymer nanocomposites for strain levels of 0.1%, 0.4%, 0.7%, and 1.0% respectively. In the nanocomposites the CNTs are well dispersed, aligned and have high aspect ratios.

3.2 Results for the axial direction of the nanocomposites

Similar to the transverse piezoresistive effect, the impact of the changes in resistivity within the CNT on the macroscale effective resistivity of the nanocomposite are provided in Fig. 4 for each of the 5 CNT gauge factors considered in Table 2. It can be seen that as the gauge factor of the CNT increases from 3E3 to 1E17, the effective resistivities tends to become bigger for the same boundary strain and the curves for the effective resistivity tend to change from linear to nonlinear with the applied boundary strain ε_0.

By applying Eq. (3), the effective gauge factors of the strain gauge with the change of boundary strain can be obtained and are shown in Table 5. It can be observed that the effective gauge factors of the strain gauge measured in the axial direction demonstrate a nearly strain independent response for the cases 1 to 3 indicating a linear macroscale piezoresistive response (the gauge factor is constant) and an increasingly strain dependent response for cases 4 and 5 indicating a non-linear macroscale resistivity-strain response. Also notice that herein only inherent piezoresistive effect of the CNT has been considered, and only in the first case is the piezoresistive coefficient of the CNT used associated with a CNT gauge factor found in the literature. However this CNT response yields a nanocomposite gauge factor nearly the same as the one induced solely by geometric effect, which is 1.54-1.55 as the strain increases from 0% to 1%. From literature review, it is found the gauge factor measured in the axial direction of the strain gauge made of 0.5%wt MWCNT that aligned by AC electric field is 2.78 ± 0.42 [5], which is comparable to the effective gauge factor obtained in case 3. Thus it can be observed that increasing the piezoresistive strain coefficient of CNT leads to the gauge factor of the nanocomposites which is on the order of those reported in the literature for case 3, and well beyond those values for cases 4 and 5. This implies that either the gauge factor/piezoresistive strain coefficient of the CNT should be larger than has been thus far reported, or that there are other factors affecting the macroscale piezoresistive response of nanocomposites such as electrical tunneling effect or contact resistance between two adjacent CNTs.

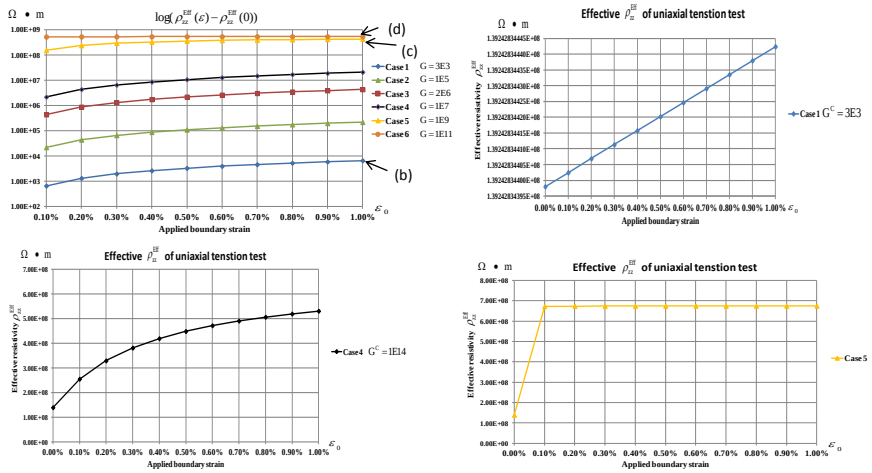

Figure 4. The effective resistivities ρ_{zz}^{Eff} with the change of strain. (a) is plot for the change of the effective resistivities ρ_{zz}^{Eff} with the applied boundary strain in semi-log plot for the 5 cases. (b), (c), and (d) are the plots for the effective resistivities ρ_{zz}^{Eff} with the applied boundary strain in linear plot for case 1, 4 and 5 respectively.

Case#	0.1%	0.4%	0.7%	1%
1	1.54	1.55	1.55	1.55
2	1.54	1.55	1.55	1.55
3	2.61	2.61	2.62	2.63
4	833.42	506.94	365.72	286.84
5	3836.00	967.34	556.22	391.78

Table 5. The effective gauge factors G^{Eff} of the strain gauge made of CNT-polymer nanocomposites for strain levels of 0.1%, 0.4%, 0.7%, and 1.0% respectively. In the nanocomposites the CNTs are well dispersed, aligned and have aspect ratio of 300.

4 CONCLUSIONS

Plane-strain and axisymmetric computational finite element models are constructed to model the transverse and axial piezoresistive response of the CNT-polymer nanocompoistes due to the inherent piezoresistive effect of CNTs, which are assumed to be well dispersed, aligned, and perfectly bonded to adjacent polymers. Quantitative results are generated and compared with experimental results in the literature. The results suggest that if the macroscale piezoresistive response of the nanocomposites is solely induced by inherent piezoresistive effect of CNTs, then in order to be comparable with experimental results, the gauge factor of the CNT needs to be as large as 1E11. Although there is literature reporting very large gauge factors of the CNT[10, 20] in the range of 1E3 to 1E4 within the strain level of 1%, such CNT gauge factors would only yield nanocomposite gauge factors on the same level as the ones induced by geometric effect. Therefore the analysis implies that the piezoresistive response of the CNT-polymer nanocomposites is more likely due to additional mechanisms, e.g. electrical tunneling effect or contact resistance between two adjacent CNTs.

References

[1] Zhang, W., Suhr, J., and Koratkar, N., Carbon nanotube/polycarbonate composites as multifunctional strain sensors, *Journal of Nanoscience and Nanotechnology*, **6**, 960-964 (2006).

[2] Kang, I., Schulz, M., Kim, J., Shanov, V., and Shi, D., A carbon nanotube strain sensor for structural health monitoring, *Smart Materials and Structures*, **15**, 737-748 (2006).

[3] JIN HO KANG, CHEOL PARK, J. A. S. . A. H. B. N. M. H., Piezoresistive characteristics of single wall carbon nanotube/polyimide nanocomposites, *Journal of Polymer Science B*, **47**, 994 -1003 (2009).
[4] Bautista-Quijano, J., Aviles, F., Aguilar, J., and Tapia, A., Strain sensing capabilities of a piezoresistive mwcnt-polysulfone film, *Sensors and Actuators A* **159**(2), 135-140 (2010).
[5] A.I. Oliva-Aviles, F. Aviles, V. S., Electrical and piezoresistive properties of multi-walled carbon nanotube/polymer composite films aligned by an electric field, *Carbon*, **49**, 2989-2997 (2011).
[6] Chunyu Li, E. T. T. and Chou, T.-W., Dominant role of tunneling resistance in the electrical conductivity of carbon nanotubebased composites, *Applied Physics Letters*, **91**, 223114-1 to 223114-3 (2007).
[7] Patrik Fernberg, Greger Nilsson, R. J., Piezoresistive performance of long-fiber composites with carbon nanotube doped matrix, *Journal of Intelligent Material Systems and Structures*, **20**, 1017-1023 (2009).
[8] Peng, S. and Cho, K., Chemical control of nanotube electronics, *Nanotechnology*, **11**, 57-60 (2000).
[9] Chen, Y.-R. and Weng, C.-I., Electronic properties of zigzag carbon nanotubes under uniaxial strain, *Carbon*, **45**(8), 1636-1644 (2007).
[10] Cullinan, M. A. and Culpepper, M. L., Carbon nanotubes as piezoresistive microelectromechanical sensors: Theory and experiment, *Physical Review B*, **82** (2010)
[11] M. P. Anantram, J. H. and Lu, J. P., Band-gap change of carbon nanotubes: Effect of small uniaxial and torsional strain, *PHYSICAL REVIEW B*, **60**(19), 874-878 (1999).
[12] Tombler, T., Zhou, C., Alexseyev, L., Kong, J., Dai, H., Liu, L., Jayanthi, C., Tang, M., and Wu, S.-Y., Reversible electromechanical characteristics of carbon nanotubes under local-probe manipulation, *Nature*, **405**, 769{772 (2000).
[13] C. Stampfer, A. Jungen, R. L. D. O. S. R. and Hierold, C., Nano-electromechanical displacement sensing based on single-walled carbon nanotubes, *Nano Letters*, **6**(7), 1449-1453 (2006).
[14] Hammerand, D., Seidel, G., and Lagoudas, D., Computational micromechanics of clustering and interphase effects in carbon nanotube composites, *Mechanics of Advanced Materials and Structures*, **14**, 277-294 (2007).
[15] Seidel, G. and Lagoudas, D., Micromechanical analysis of the effective elastic properties of carbon nanotube reinforced composites, *Mechanics of Materials*, **38**(8-10), 884-907.
[16] Seidel, G. and Lagoudas, D., A micromechanics model for the electrical conductivity of nanotube-polymer nanocomposites, *Journal of Composite Materials*, **43**(9), 917-941 (2009).
[17] Ebbesen, T., Lezec, H., Hiura, H., Bennett, J., Ghaemi, H., and Thio, T., Electrical conductivity of individual carbon nanotubes, *Nature*, **382**, 54-56 (1996).
[18] Schadler, L., Giannaris, S. C., and Ajayan, P. M., Load transfer in carbon nanotube epoxy composites, *Applied Physics Letters*, **73**(26), 3842-3844 (1998).
[19] Arris, H. W., An overview of high reliability transformer encapsulation materials, *tech. rep.*, Sandia National Laboratories (2000).
[20] Hierold, C., Jungen, A., Stampfer, C., and Helbling, T., Nano electromechanical sensors based on carbon nanotubes, *Sensors and Actuators A*, **136**(1), 51-61 (2007).